Journal of Chemical Health Risks

www.jchr.org

JCHR (2026) 16(1), 2509-2515 | ISSN:2251-6727

Wavelet Coherence Analysis of Brain and Muscle Electrical Activities in Lower Limb Movements

Avanish Kumar Singh 1 , Sivakumaran N 1 , and Arunganesh K 2 , Kumaravel S 3

1 Department of Instrumentation and Control Engineering, National Institute of Technology, Tiruchirappalli, Tamil Nadu, India.

2 Department of Electrical and Electronics Engineering, Thiagarajar College of Engineering, Madurai, Tamil Nadu, India.

3 Government Hospital, Trichy-620001, Tamil Nadu, India

(Received: 05 December 2025 Revised: 15 January 2026 Accepted: 10 February 2026)

KEYWORDS

EEG, EMG, Corticomuscular coherence (CMC) and Wavelet coherence.

ABSTRACT:

Corticomuscular coherence (CMC), which represents the link between the electroencephalogram (EEG) and the electromyogram (EMG), is frequently used to investigate the functional relationship between the human brain and muscles. The wavelet coherence function will be used in this study to evaluate EEG-EMG coherence. Datasets comprising simultaneous EEG-EMG signals from ten subjects walking on flat surfaces, stairs, and ramps that are publicly accessible are used. EEG signals from the motor cortex region (C1, C2, and CZ) and EMG signals from the tibialis anterior (TA) are subjected to the wavelet coherence function. The paper looks at how the theta (0.5–4 Hz), delta (4–8 Hz), alpha (8–12 Hz), beta (14–30 Hz), and gamma (30–50 Hz) frequency bands interact with the EEG and EMG signals. The results reveal a notable coherence across a variety of activities between the electrical activity of the brain and that of the muscular system. Various activities also show various frequency-band interactions. The Kruskal-Wallis non-parametric one-way ANOVA test is used to assess the statistical significance of the results, which reveals that during level walking activities the theta and alpha frequency bands and coherence values in the C2-TA and CZ-TA groups are significantly higher than those in the control group ($p < 0.05$) Still, none of the three channels show notable numbers in the other frequency range. Still, none of the three channels show significant data in the other frequency range. Especially in the alpha frequency range (8–12 Hz), the results showed that C1-TA had an MSC level of 3.12 for the highest coherence levels. Natural techniques are used in this work to cover all typical frequency bands. Results for different walking patterns across separate EEG channels show that the theta and alpha frequency bands have considerably stronger coherence than the others. This is pertinent to clinical methods of CMC analysis and provides fascinating content for further CMC research.

1. INTRODUCTION

An essential question in the neurological study is how the human brain recognizes, processes, and acts on the massive quantity of information that flows through it seemingly effortlessly. Although the physiological structure of the brain is fairly well-defined, the fundamental system that allows its numerous parts to work in combination has not yet been discovered. However, understanding the brain and establishing correlations between different muscles is an extremely complicated challenge since it contains billions of neurons interconnected by trillions of connections. Efforts in this area have focused on various levels of the human brain, varying from the level of molecules, which involves recognizing physiological relationships between neurons and muscle information, to the system level, which models information flows between groups of neurons and psychological activities.

Corticomuscular coherence (CMC) [1] is a well-liked and potent tool for probing the mechanism of muscular activity modulation by cerebral cortex. It describes how the brain and muscles work together to maintain continuous muscular contractions. The interaction between primary motor cortex and muscle in the corticospinal pathways is the source of CMC.

In a normal situation, activities that take place in the cortex will spread out to the periphery, and the motor cortex will also receive information from the peripheral [2, 5]. The several technics have been explored for EEG-EMG coupling analysis includes cortical–muscular functional coupling [6, 7], granger causality analysis [8, 9], transfer entropy (TE) analysis [10, 11], symbolic transfer entropy (STE) analysis [12], magnitude squared coherence (MSC) [13] and wavelet coherence (WT) [14]. Among these, wavelet coherence and symbolic transfer entropy methods are often used for better coherence analysis in various aspects. The primary benefit of wavelet coherence method is that frequency bands are segmented automatically, without the need to specify frequency levels.

The corticomuscular coherence (CMC) between lower limb muscles and the motor cortex is important to explain the neural mechanisms that support voluntary motor control. Arun Ganesh et al. probed this inter-relationship based on Symbolic Transfer Entropy (STE) for examining information flow directionally from the motor cortex to Tibialis Anterior muscle. Their findings indicated a significant directional interaction, emphasizing the close coordination of cortical and muscle activity necessary for precise motor execution and useful in neurorehabilitation environments [2].This group performed another analysis of CMC in the communication between broader cortical and lower limbs muscles through the use of EEG and EMG recordings. It showed high coherence, especially of the beta band frequency (13–30 Hz), which was linked to the planning and production of motor events. This article reiterates the importance of corticomuscular synchronization with voluntary movement and lays a background for the future formulation of specifically aimed therapeutic remedies for motor dysfunctions [3].

The wavelet transform allows for the measurement of frequency domain features at a variety of resolutions. To capture the temporal and frequency-specific characteristics of non-stationary signals, analytical methods in the time-frequency domain, such as wavelet coherence [15, 16], prove effective in addressing the challenges mentioned above. Wavelet coherence is a recently developed technique to examine such coherence in a very straightforward yet accurate approach. Essentially, two time series are compared after being converted to wavelets. The ability to filter out signals into wavelets through a window and just use the necessary portion of the signal as an input is one benefit of wavelet transformation.

In this study, efforts were directed towards gauging EEG-EMG coherence through wavelet coherence analysis. The study examined wavelet coherence between lower limb muscle EMG data and EEG signals from the main motor brain. All default frequency bands are covered in this work. Especially in channels C2 and CZ, the findings showed notable values mostly in the alpha frequency areas. These results are important for therapeutic strategies for neuromuscular diseases and offer useful guidance for CMC future research as well. The paper is structured as follows: The second part explains the wavelet coherence and dataset technique. Results are summarized in Section 3 along with a short explanation of our method. At last, Section 4 wraps up and suggests next steps for this study.

2. MATERIALS AND METHODS

2.1 Dataset

The study's findings show utilized a publicly accessible comprehensive mobile brain-body imaging database [17]. Ten participants, comprising five males and five females aged between 18 and 31 years, engaged in diverse walking activities, including stair and ramp walking. EEG signals were recorded using a 64 channel 10-20 electrode system with 1000 Hz of sampling frequency. Surface EMG signals were captured with active bipolar electrodes at 1000 Hz, focusing on six lower limb muscles. The study specifically examined EEG contacts related to the primary motor cortex area, specifically C_Z, C_1, and C_2, along with EMG signals from the tibialis anterior (TA) muscle. Analysis encompassed the interaction of conventional EEG frequency bands; delta (0.2 - 4 Hz), theta (4 - 8 Hz), alpha (8 - 12 Hz), beta (12 - 30 Hz), and gamma (30 - 50 Hz) and the spectral components of both EEG and EMG signals. Custom programs were

Journal of Chemical Health Risks
www.jchr.org
JCHR (2026) 16(1), 2509-2515 | ISSN:2251-6727

developed in the MATLAB version 2017b environment for this purpose.

2.2 Wavelet Coherence

To capture the non-linear characteristics of enhanced EEG-EMG coherence, the analysis employs wavelet coherence. This method leverages the features of wavelet transform, increasing the signal for analysis in the temporal and frequency domain, which is absolutely vital for non-stationary signals. In this context, wavelet the processed EEG signal is decomposed by wavelet analysis into sub-signals in several frequency bands. Using frequency bands that govern muscular activity, wavelet coherence analysis in the time-frequency domain on the EMG data follows this.

We suggest that x(t) and y(t) are time series respectively for EMG and EEG signals. The convolution of the generalized wavelet function Ω(t) with x(t) produces the wavelet factors for the signal x(t), indicated as W(m, n).

$$W_x(\mathrm{m,n}) = \left(\mathrm{x}, \Omega_{m,n}\right) = \frac{1}{\sqrt{m}} \int_{-\infty}^{\infty} x(t)\, \Omega * \left(\frac{t-n}{m}\right) dt \quad (1)$$

Here, 'm' is the wavelet scale, inversely connected to frequency; 'n' is smoothing; 't' is the local time origin in wavelet analysis; '*' denotes conjugation; Ω ((t-n)/m) is the wavelet basis function. For this specific study, the Morlet wavelet is employed.

We found the cross-wavelet transformation of x(t) and y(t) as $|W_{yx}(m,n)|$ is

$$\left|W_{yx}(\mathrm{m,n})\right| = \left|W_y(m,n) W_x * (m,n)\right| \quad (2)$$

In order to acquire comprehensive synchronization details for both signals, it is essential to smooth the wavelet spectrum before computing the wavelet coherence. Following the wavelet transformation, Refining the signal depends much on the smoothing function. The design of the smoothing function is

$$S(\mathrm{W}) = S_m\left[S_t(W)\right] \quad (3)$$

Here, S_m represents m smoothing process along the measure axis,

$$S_m(\mathrm{W(m,n)}) = \mathrm{W(m,n)} * F_1 \prod(0.6m) \quad (4)$$

S_t signifies a smoothing process along the time axis,

$$S_t(\mathrm{W(m,n)}) = \mathrm{W(m,n)} * F_2^{-\frac{t^2}{2m^2}} \quad (5)$$

In this context, F_1 and F_2 represent normalization coefficients, with a possible setting of 0.9; '*' denotes the convolution control. Consequently, the coefficients for wavelet coherence between the following expresses (t) and x(t),

$$Wco_{yx}(\mathrm{m,n}) = \frac{\left|S\left(W_{yx}\ (m,n)\right)\right|}{\sqrt{S(|W_Y(m,n)|^2) S(|W_X(m,n)|^2)}} \quad (6)$$

The range of the wavelet coherence factor is 0 to 1. Strong coherence is indicated by a number near to 1, whereas poor coherence is indicated by a value closer to 0.

3. RESULTS AND DISCUSSION

The representation EEG signals of subject 1 shown in Figure 1 in the amplitude range from 0 to 2 µV and the amplitude range of EMG signals between 0 to 2 mV with maximum walking duration of 20 sec based on walking activities.

Journal of Chemical Health Risks
www.jchr.org
JCHR (2026) 16(1), 2509-2515 | ISSN:2251-6727

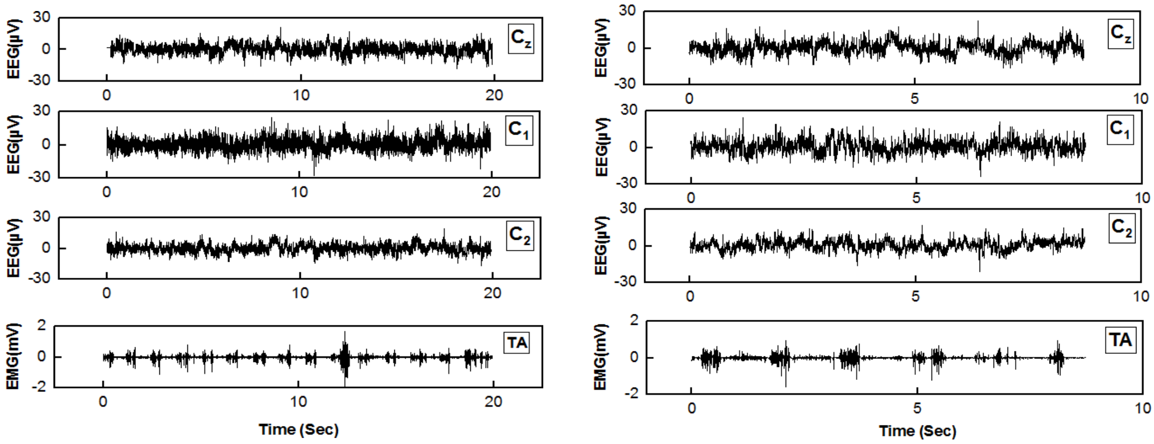

(a) (b)

Figure 1: Representative EEG (C_1, C_2 and C_Z) and EMG (TA) signals: (a) level walking (b) walking on stair

The Figure 2 shows the wavelet coherence between an EEG and EMG signal of a subject of three channels (C_1, C_2 and C_Z) with TA muscle during the level walking activities. The x axis denotes the time period which is generated based on the sampling frequency (1000 Hz) and the y axis denotes the periodic frequency along the time series.

A **B** **C**

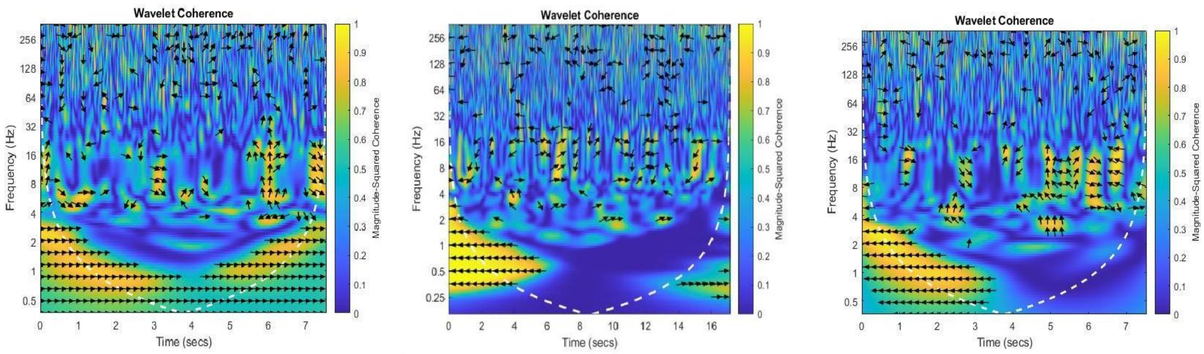

Fig. 2 Wavelet coherence of level ground walking task; (A) C_1 and TA (B) C_2 and TA (C) C_Z and TA

The dotted is known as the Cone of Influence (COI) which represents the area in which there is actual coherence, the coherence shown outside the cone of influence are noise and artifacts. The color bar from blue to yellow represents amplitude of magnitude squared coherence from the scale of 0 to 1. The arrows, referred to as phase arrows, signify the phase shift in the coherence between the EMG and EEG signal. The yellow shaded regions in Figure 2 depict robust simulations of EEG-EMG coherence. It is evident that the frequency band and duration of substantial coherence vary across these figures, corresponding to different EMG response times. According to the results, Figures 2A demonstrate the highest coherence levels, particularly in the alpha frequency band, registering a coherence level of 3.12 for C1-TA. Furthermore, Figures 2A and 2B, corresponding to level walking and walking on stair activities, reveal some coherence in the beta band with coherence values of 2.66 and 2.78, respectively.

Journal of Chemical Health Risks
www.jchr.org
JCHR (2026) 16(1), 2509-2515 | ISSN:2251-6727

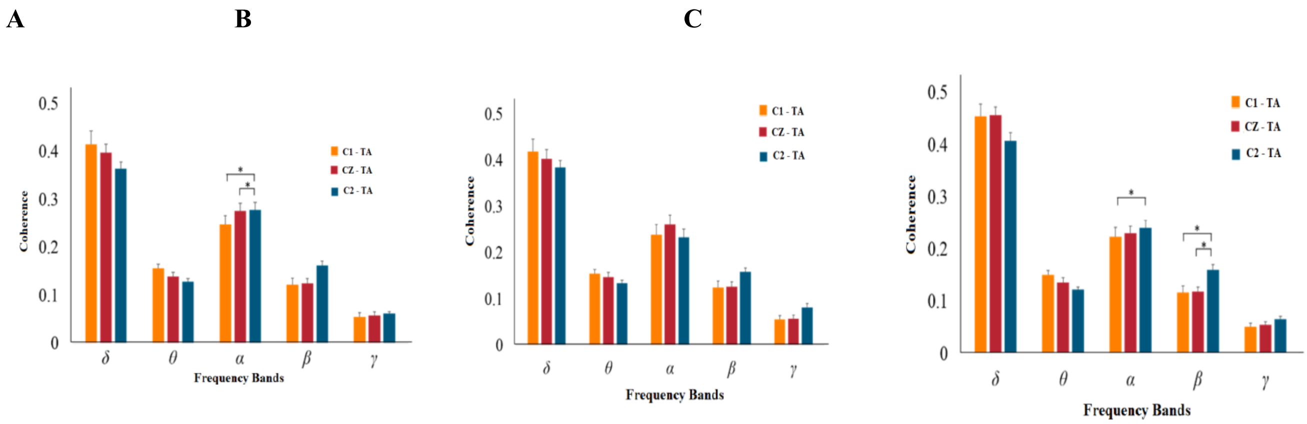

Figure 3.Statically analysis of wavelet coherence: (A) level walking (B) walking on ramp(C) walking on stair.

Statistical significance was evaluated using the Kruskal-Wallis non-parametric one-way ANOVA test comparing different frequency bands across independent observations related to major activities, namely level walking, waling on ramp, and walking on stair. The outcomes of wavelet coherence analysis for channels C_1 and C_2, focusing on the delta and alpha frequency bands as illustrated in Figure 3A, exhibited noteworthy distinctions. Particularly in the alpha frequency band, during level walking exercises, coherence values in the C2-TA and Cz-TA groups were significantly higher than those in the control group ($p < 0.05$). Still, over all three channels in the other frequency bands, no statistically significant values were observed. Figure 3C outlines the wavelet coherence during walking on ramp activities across various frequency bands, with the highest coherence again observed in the delta and alpha frequency bands.

However, no significant values were found in any frequency bands during these activities. Notably, in the β frequency band, coherence values during ramp walking activities were generally lower than those in walking and stair walking activities across most channels. In channels C_1 and C_2, the alpha frequency band during ramp walking showed a significant decrease compared to other activities. Significant differences were also observed in the stair walking activities across all channels, specifically in the alpha frequency band ($p < 0.05$), as depicted in Figure 3C. In the gamma frequency band, coherence values decreased in all three channels, with no significant differences noted during these activities. Ultimately, the findings indicate that significant values were predominantly confined to the alpha frequency bands, especially in the C_2 and Cz channels. This is pertinent for clinical methods to Corticomuscular Coherence (CMC) study and provides insightful analysis for coming CMC studies.

4. CONCLUSIONS

This study introduces a wavelet coherence based CMC analysis, building upon the magnitude squared coherence (MSC) approach. This study uses natural techniques to include all typical frequency bands. Results are shown for different walking activities across separate EEG channels, hence stressing especially greater coherence in the alpha and theta frequency bands relative to others. Noteworthy variances were detected during stair walking activities across all channels, particularly in the alpha frequency band ($p < 0.05$). This work offers extensive findings that advance the diagnosis of neuromuscular disorders and play a role in brain-computer interfaces (BCI) for rehabilitation purposes. Moreover, these corticomuscular coherence (CMC) findings lay the groundwork for potential future applications in wearable sensor technology. The future research should incorporate bilateral analysis for a more comprehensive approach. Furthermore, expanding the number of muscles considered can significantly enhance the overall performance of CMC applications.

Financial support and sponsorship

Nil.

Conflicts of interest

There are no conflicts of interest.

REFERENCES

1. Kilner, J. M.; Baker, S. N.; Salenius, S.; Hari, R.; Lemon, R. N. Human cortical muscle coherence is directly related to specific motor parameters. *J. Neurosci.* **2000**, *20*, 8838–8845. https://doi.org/10.1523/JNEUROSCI.20-23-08838.2000.

2. Riddle, C. N.; Baker, S. N. Manipulation of peripheral neural feedback loops alters human corticomuscular coherence. *J. Physiol.* **2005**, *566*, 625–639. https://doi.org/10.1113/jphysiol.2005.089607.

3. Arun Ganesh, K.; Vinothini, S.; Sivakumaran, N.; Kumaravel, S.; Karthick, P. A. Analysis of corticomuscular coherence between motor cortex region and tibialis anterior muscle using symbolic transfer entropy. In *Proceedings of the IEEE International Symposium on Medical Measurements and Applications (MeMeA)*; IEEE: **2022**.

4. Arun Ganesh, K.; Sivakumaran, N.; Kumaravel, S.; Karthick, P. A. Analysis of corticomuscular coherence between cortical and lower limb muscle activities. *J. Biomed. Sci. Instrum.* **2021**, *57* (3).

5. Gross, J.; Tass, P. A.; Salenius, S.; Hari, R.; Freund, H. J.; Schnitzler, A. Cortico-muscular synchronization during isometric muscle contraction in humans as revealed by magnetoencephalography. *J. Physiol.* **2000**, *527*, 623–631. https://doi.org/10.1111/j.1469-7793.2000.00623.x.

6. Poortvliet, P. C.; Tucker, K. J.; Finnigan, S.; Scott, D.; Sowman, P.; Hodges, P. W. Cortical activity differs between position- and force-control knee extension tasks. *Exp. Brain Res.* **2015**, *233* (12), 3447–3457. https://doi.org/10.1007/s00221-015-4404-8.

7. Cremoux, S.; Tallet, J.; Dal Maso, F.; Berton, E.; Amarantini, D. Impaired corticomuscular coherence during isometric elbow flexion contractions in humans with cervical spinal cord injury. *Eur. J. Neurosci.* **2017**, *46* (4), 1991–2000. https://doi.org/10.1111/ejn.13641.

8. Hu, S.; Wang, H.; Zhang, J.; Kong, W.; Cao, Y. Causality from Cz to C3/C4 or between C3 and C4 revealed by Granger causality and new causality during motor imagery. In *Proceedings of the International Conference on Neural Networks*; **2014**; pp 3178–3185. https://doi.org/10.1109/TNNLS.2015.2441137.

9. Tomasevic, L.; Zito, G.; Pasqualetti, P.; Filippi, M.; Landi, D.; Ghazaryan, A.; et al. Corticomuscular coherence as an index of fatigue in multiple sclerosis. *Mult. Scler.* **2013**, *19* (3), 334–343. https://doi.org/10.1177/1352458512452921.

10. Ping, X.; Yang, F. M.; Li, X. X.; Yong, Y.; Chen, X. L.; Zhang, L. T. Functional coupling analyses of electroencephalogram and electromyogram based on variational mode decomposition–transfer entropy. *Acta Phys. Sin.* **2016**, *65* (11), 118701. https://doi.org/10.7498/APS.65.118701.

11. Vicente, R.; Wibral, M.; Lindner, M.; Pipa, G. Transfer entropy—a model-free measure of effective connectivity for the neurosciences. *J. Comput. Neurosci.* **2011**, *30* (1), 45–67. https://doi.org/10.1007/s10827-010-0262-3.

12. Yao, W.; Wang, J. Multi-scale permutation transfer entropy analysis of EEG. *Physica A* **2017**, *484*, 276–281. https://doi.org/10.3389/fneur.2017.00716.

13. Bortel, R.; Sovka, P. EEG and EMG coherence enhancement. *Signal Process.* **2006**, *86*, 1737–1751. https://doi.org/10.1016/j.sigpro.2005.09.011.

14. Chavez, M.; Cazelles, B. Detecting dynamic spatial correlation patterns with generalized wavelet coherence and non-stationary surrogate data. *Sci. Rep.* **2019**, *9*, 7389. https://doi.org/10.1038/s41598-019-43571-2.

Journal of Chemical Health Risks
www.jchr.org
JCHR (2026) 16(1), 2509-2515 | ISSN:2251-6727

15. Schaefer, L. V.; Bittmann, F. N. Coherent behavior of neuromuscular oscillations between isometrically interacting subjects: Experimental study utilizing wavelet coherence analysis of mechanomyographic and mechanotendographic signals. *Sci. Rep.* **2018**, *8* (1), 15456. https://doi.org/10.1038/s41598-018-33579-5.

16. Ieracitano, C.; Duun-Henriksen, J.; Mammone, N.; La Foresta, F.; Morabito, F. C. Wavelet coherence-based clustering of EEG signals to estimate brain connectivity in absence epileptic patients. In *Proceedings of the International Joint Conference on Neural Networks (IJCNN)*; **2017**. https://doi.org/10.1109/IJCNN.2017.7966002.

17. Brantley, J. A.; Luu, T. P.; Nakagome, S.; Zhu, F.; Contreras-Vidal, J. L. Full body mobile brain–body imaging data during unconstrained locomotion on stairs, ramps, and level ground. *Sci. Data* **2018**, *5*, 180133. https://doi.org/10.1038/sdata.2018.133.